Quantitative description of the microstructure of duplex stainless steels using selective etching

Fedorov A.[1], Zhitenev A.[1*], Strekalovskaya D.[1], Kur A.[1]

[1]Peter the Great St. Petersburg Polytechnic University

Russia, 195251, St. Petersburg, Polytechnicheskaya, 29

e-mail: zhitenev_ai@spbstu.ru

Abstract

The properties of duplex stainless steels (DSSs) depend on the ferrite-austenite ratio and on the contents of secondary phases. Therefore, it is necessary to control the volume fractions, morphologies and distribution patterns of all phases. The phases in the samples were identified using thermodynamic modeling and scanning electron microscopy. Investigated specimens were obtained after different heat treatments, such as solution annealing and quenching from 1050-1250 °C to obtain different amounts of ferrite and annealing at 850 °C to precipitate σ-phase. Therefore, a metallographic technique for assessing the phases in DSSs based on selective etching and subsequent analysis according to ASTM E 1245 was developed. It was shown that the developed method of quantitative analysis based on selective etching and metallographic assessment according to ASTM E 1245 allows obtaining a much more accurate results compared to the proposed ASTM E 562 method, which correlates well with the XRD quantitative phase analysis.

Keywords: duplex stainless steel, δ-ferrite, austenite, σ-phase, etching, quantification

Introduction

The properties of duplex stainless steels (DSSs) depend on a ferrite-austenite ratio and on contents of secondary phases [1]. The actual phase content depends on the chemical composition of the steel, and heat treatment of the final product [2]. Therefore, it is necessary to control the volume fractions, morphologies and distribution patterns of all phases. The existing physical methods of assessing phases volume fractions, such as magnetic response or X-ray diffraction (XRD) quantitative phase analysis, work either with reference to certain databases to interpret the results, or in very narrow determination ranges [3, 4]. These methods also require preparation of additional specimens, while metallographic assessment can be carried out using only specimens made after mechanical tests. There is a wide range of metallographic standards and methods for assessing grain size [5], non-metallic inclusions content [6] and microstructural banding [7] for carbon steels. However, there are few such standards for DSSs. Therefore, the aim of this work was a development of metallographic technique for assessing the phases in DSSs, based on selective etching and subsequent analysis according to ASTM E 1245.

Materials and methods

In this study specimens of as-cast duplex steels of different grades were investigated (Table 1, Steels 1, 2, 3, 4). The specimens were examined after different heat treatments. The experimental steel was produced in the open induction furnace [8]. The raw materials were high-purity electrical steel, metallic chromium, metallic nickel, ferromanganese-95 and ferromolybdenum-60. After heating and melting at 1485 °C, liquid steel was poured into a cylindric copper mold with a diameter of 40 mm and a height of 100 mm. The chemical composition of the experimental steels was determined by a spark optical emission spectroscopy. The content of sulfur and phosphorus in all steels did not exceed 0.01%.

Table 1 – Chemical compositions of experimental steels

Steel	Element, wt.%								
	C	Si	Mn	Ni	Mo	N	Cu	Ti+Nb+V	Cr
1	0.02	0.6	1.6	6	0.50	0.04	0.17	0.06	21
2									23
3									26
4	0.03	0.5	1.0	6	4.00	0.20	2.50	0.10	23

The samples of steel were heat treated in the programmable muffle furnace: heated to different temperatures of 1050-1250 °C with a step of 50 °C, held at each temperature for 60 minutes, and quenched in water. In Steel 4 the formation of a σ-phase is possible [9]. To form various contents of a σ-phase, samples of Steel 4, were subjected to annealing at a temperature of 850 °C for 15-120 minutes.

Heat-treated steels were used to produce metallographic specimens by molding it in a phenolic compound, grounding and polishing. The structures of these specimens were revealed using various etchants.

Metallographic studies were performed using light optical microscopy method. Microstructure was investigated using the inverted Reichert-Jung MeF3A microscope equipped with a Thixomet Pro image analyzer.

The chemical composition of each phase was studied using a Zeiss Supra scanning electron microscope equipped with an energy dispersive spectrometer. To confirm the results of quantitative metallography, the phase content in the same specimens were determined by Bruker's X-ray diffractometer. Thermodynamic modeling was carried out by the ThermoCalc software package with the TCFE database [10].

DSS's etchants overview

Numerous works are known in which one or another reagent was used [11-15] to reveal the structure of DSSs (Table 2). However, there is no unified approach that allows a sufficiently accurate quantitative assessment of the DSS's structure. The well-known method for determining volume fraction by systematic manual point count allows measurement of the amount of ferrite or austenite even with low etching quality. Modern image analyzers can significantly increase the accuracy and speed of measurements, provided that an image of the structure is suitable for recognition. Table 2 lists the most common reagents used to identify the structure of DSSs. The articles describe different applications of these reagents. For example, etching with the Murakami etchant was used in [11]; however, in [12], it was shown that, it is rather difficult to identify ferrite if its fraction is small using such etching. Another equally important issue is the selective etching of the σ-phase. The most common method for its recognition is XRD, and there is no definite etchant for its revealing [11, 13, 14], as well as for other harmful phases in DSSs.

Table 2 – Used etchants and features of their application

№	Name	Composition	Notes	Ref.
Chemical etching				
1	Inhibited ferric chloride	100 mL water, 5 g $FeCl_3$, 1 g $NaNO_3$	It identifies detrimental phases in lean DSSs	[15]
2	Sodium Hydroxide	100 mL water, 40 g NaOH	It identifies detrimental phases	[11]
3	Modified Beraha (Beraha's sulfamic acid reagent No. 4)	100 mL water, 3 g $K_2S_2O_5$, 2 g sulfamic acid, 0,5-1 g NH4F · HF	It identifies phases in high-alloy steels upon immersion for 30-180 s	[14]
4	Beraha	20 mL HCl, 80 mL water, 1 g $K_2S_2O_5$	It reveals ferrite. Etch by immersion until formation of tint	[12,14]
5	Carpenter	85 mL ethanol, 15 mL HCl	It identifies grain boundaries and σ-phase. Etch by immersion for 15-45 minutes	[12,14]
6	Murakami	100 mL water, 10 g NaOH, 10 g $K_3Fe(CN)_6$	It reveals ferrite when heated up to 80-100 °C, reveals carbides at room temperature	[13,14]
7	"Glyceregia"	15 mL HCl, 10 mL glycerol, 5 mL HNO_3	It reveals grain boundaries and σ-phase	[11]
Electrolytic etching				
8	HNO_3	60% nitric acid	It identifies ferrite and σ-phase when etched at 2.2 V for 10 s	[13]
9	NaOH	100 mL water, 20 g NaOH	It identifies ferrite and σ-phase when etched at 3 V for 10 s	[14]

Etching method development

To develop a quantitative assessment technique, it is necessary to select an etchant that allows obtaining a contrast image of phases for automatic analysis. The structure of the specimen of Steel 1 with 21% Cr (Table 1), quenched from a temperature of 1200 °C was investigated (Figure 1). Three Vickers indentations were made on this specimen with a load of 180 g to indicate the investigated field of view and to make an image of the revealed microstructure after each subsequent etching. In order to always observe the same structure, a polishing after each iteration was carried out with a minimal metal removal.

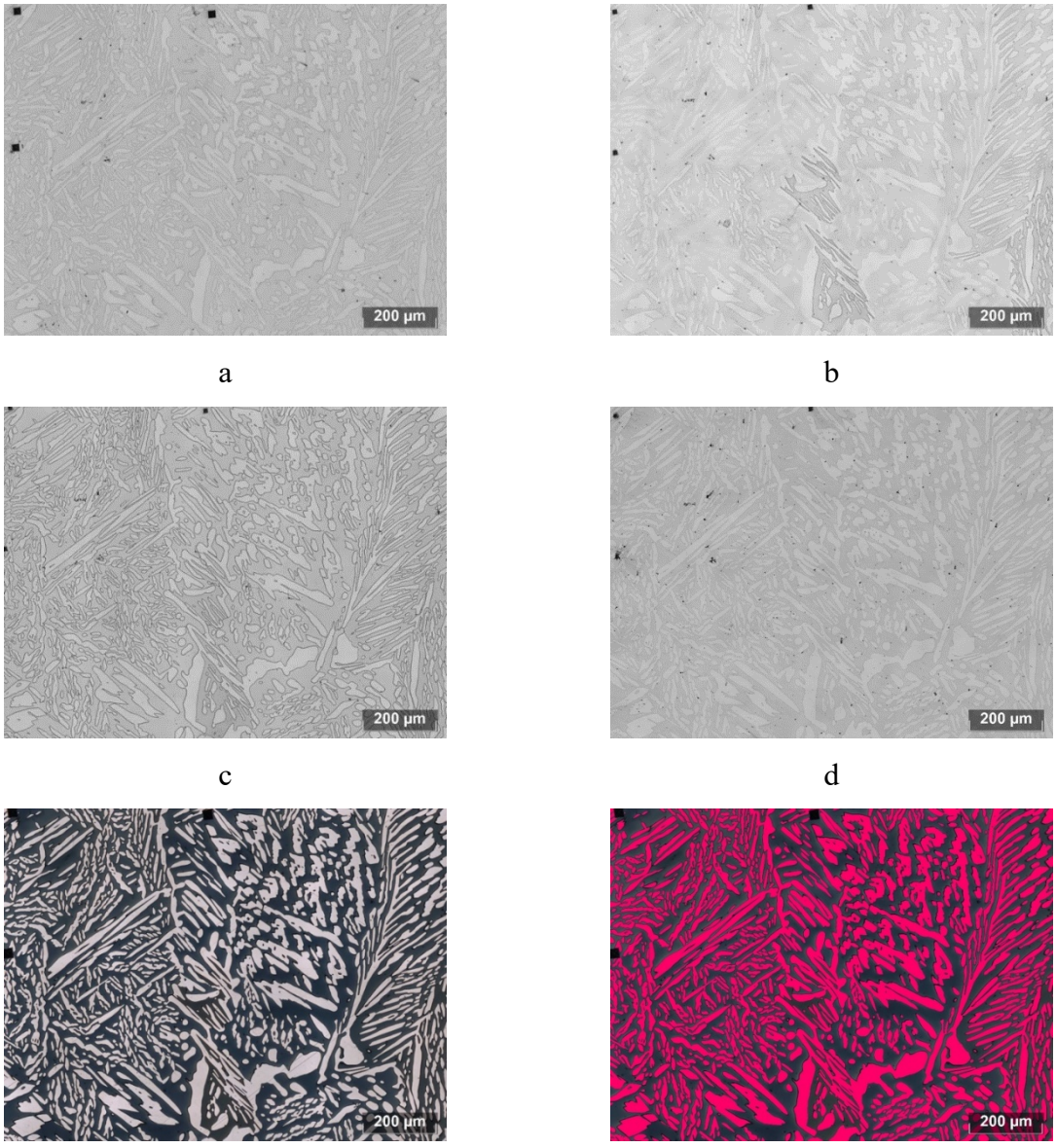

Figure 1. Microstructure of Steel 1, quenched from 1200 °C, after electrolytical etching using NaOH (a), chemical etching using Glyceregia (b), Carpenter (c), Murakami's (d), Beraha's (e) etchant solutions, and austenite automatic identification after using Beraha's (f)

Some etchants (reagents 1-3, Table 2), recommended by other authors, did not work on investigated DSSs. Thus, the chemical etching with inhibited ferric chloride and sodium hydroxide did not reveal the structure. The Modified Beraha's reagent showed a very undistinguishable structure.

Electrolytic etching is one of the most common techniques for revealing the structure of DSSs [11]. Figure 1a shows the microstructure revealed by electrolytic etching of NaOH, which consists of a dark ferrite matrix and light austenite islands [16]. Using 60% nitric acid as an electrolyte gives the same result. This etching method provides stable high-quality images of the DSS's structure, but the contrast between phases is insufficient for automatic classification by the image analyzer. Therefore, this etching technique is only suitable for measuring by manual point count method [17].

Other etchants according to Table 2 (Glyceregia in Figure 1b, Carpenter in Figure 1c, Murakami's etchant in Figure 1d) showed similar results. These etchants, similar to electrolytic etching, does not provide sufficient contrast on images for automatic quantitative description of the microstructure of DSSs. Moreover, the Murakami etchant solution requires heating to a temperature of 80-100 °C, which is unsafe and requires additional equipment.

Etching with Beraha's (reagent 4, Table 2) makes it possible to obtain a sufficient contrast of ferrite (Figure 1e), which is darkened, opposed to unetched austenite. The contrast level in grayscale is sufficient to carry out binarization at a given brightness threshold and determine the volume fraction of phases according to the ASTM E1245 standard in an automated mode (Figure 1f).

The σ-phase leads to the strengthening of DSSs and to a simultaneous decrease in corrosion properties. The reagent selection for detecting it is also an important problem. Figure 2 shows the microstructure of a specimen of Steel 4 after annealing at 850 °C. It was revealed using the Beraha's etchant (reagent 4, Table 2), which showed the best result earlier in identifying ferrite and austenite.

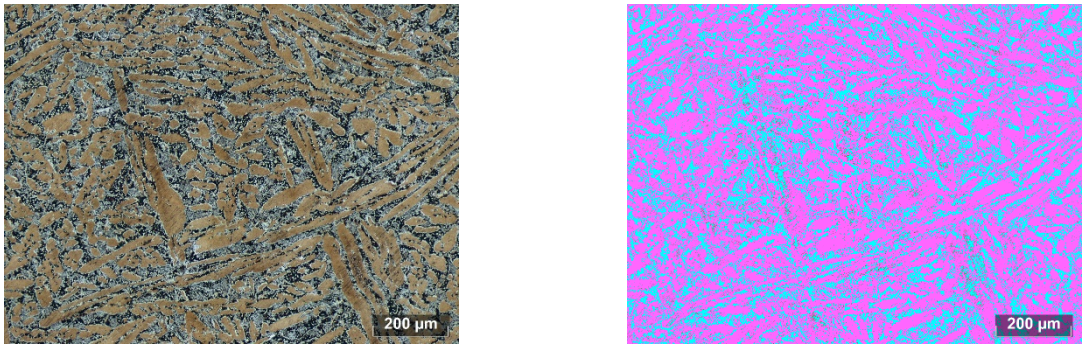

a b

Figure 2. Dark ferrite, light gray σ-phase and brown austenite (a) in Steel 4 after annealing at 850 °C for 15 minutes, and a phase identification using image analyzer (b)

This etching reveals dark areas of ferrite that has not transformed into a σ-phase (Figure 2a), light gray areas of the σ-phase, and brown austenite. The image obtained after such etching can be binarized over specified ranges and the volume fraction of each phase can be determined (Figure 2b). Volume fraction of austenite (magenta in Figure 2b) and ferrite (blue in Figure 2b) was found. The content of the σ-phase was calculated as balance.

For a more detailed interpretation of the phase nature, the local chemical composition of the specimens was determined (Figure 3, Table 3).

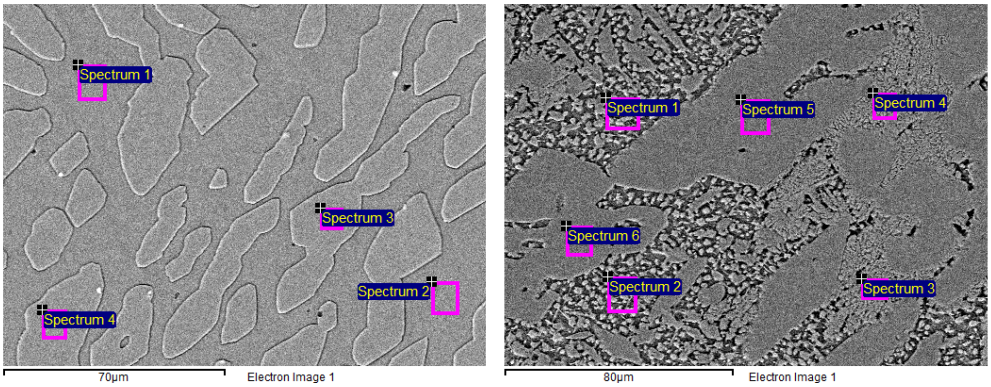

a b

Figure 3. SEM images of ferrite and austenite in Steel 1 after quenching from 1200 °C (a) and in Steel 4 after annealing at 850 °C for 15 minutes

The content of ferrite-stabilizing elements in ferrite of Steel 1, quenched from 1200 °C (Figure 3a, Table 3, lines 1, 2) was as follows: 1.9-2.5% molybdenum, 23.0-23.3% chromium and 5.4-5.7% nickel. In the contrary, a content of chromium and molybdenum in austenite (Figure 3b, Table 3, lines 3, 4) is lower (20.0-20.2% and 1.0-1.1%, respectively). The concentration of nickel in austenite is higher than in ferrite, reaching 7.2-7.5%.

The content of the remaining elements (manganese and silicon) taking into account the error in their determination is the same. In the austenite of Steel 4, which was subjected to annealing to precipitate a σ-phase at 850 °C for 15 minutes (Figure 3b, Table 3, points 5, 6), the lowest concentration of chromium and molybdenum (25% and 4.2-4.6%, respectively) was determined, but the concentration of nickel found to be the highest. In the ferrite (Figure 3b, Table 3, points 7, 8) the content of chromium and molybdenum is higher (28.2-28.5% and 5.1% respectively). In the σ-phase (Figure 3b, Table 3, points 9, 10) a chromium concentration is slightly lower than in the ferrite, and the molybdenum content is the highest, reaching 12.3-12.4%.

Thus, the proposed etching method (Beraha's etchant and automatic image analysis) makes it possible to detect austenite, ferrite and σ-phase in DSSs, and to obtain high contrast of the phases on images for automatic quantitative assessment according to ASTM E1245.

Table 3 – Chemical composition of phases in DSS's specimens

№	Spectrum (Figure 3)	Element, wt%					Phase
		Cr	Ni	Mo	Mn	Si	
Steel 1, quenched from 1200 °C (to Figure 3a)							
1	1	23.3	5.4	1.9	1.5	0.7	δ
2	2	23.0	5.7	2.5	1.5	0.8	
3	3	20.1	7.5	1.0	1.8	0.7	γ
4	4	20.2	7.2	1.1	1.6	0.7	
Steel 4, quenched from 1050 °C, annealing at 850 °C for 15 minutes (to Figure 3b)							
5	5	25.0	8.0	4.2	1.4	0.5	γ
6	6	25.0	7.7	4.6	1.4	0.6	
7	3	28.2	5.1	8.0	1.2	0.7	δ
8	4	28.5	5.1	8.1	1.1	0.6	
9	1	25.8	6.2	12.3	1.2	0.6	σ
10	2	26.0	5.8	12.4	1.2	0.7	

Analysis of DSS's specimens obtained using different heat treatments

Depending on the chemical composition and the heat treatment of the DSS, it is possible to obtain different ratios of austenite and ferrite, and also to precipitate σ-phase. The austenite content in specimens of Steels 1, 2, and 3 (Table 1), quenched from different temperatures, was determined using a technique based on etching with Beraha's reagent and image analysis (Table 4).

Table 4 – Comparison of methods for assessing the volume fraction of phase components

Steel	Quenching temperature	Austenite content		
		Automatic analysis after etching with Beraha's, vol.%	Measurements by the systematic manual point count method after electrolytic etching with NaOH, vol.%	Thermodynamic modeling, wt.%
1	1050	61.0	64.5	67.7
	1100	57.8	63.0	61.2
	1150	52.1	53.5	52.3
	1200	43.0	47.5	42.6
	1250	42.7	53.5	30.2
2	1050	44.8	58.5	51.9
	1100	39.1	46.0	45.0
	1150	27.4	27.5	36.7
	1200	18.5	15.5	26.8
	1250	15.0	7.0	15.0
3	1050	25.9	39.0	32.6
	1100	17.2	27.5	25.4
	1150	8.9	6.0	17.2
	1200	0.2	3.0	7.9
	1250	0.1	0.0	0.0

The measurement results obtained by automatic image analysis correlates with the results obtained by the manual point count method. Both methods correlate with the predicted phase contents according to thermodynamic calculations too (both weight and volume %, providing that difference in densities of the phases is negligible). However, the evaluation area and the statistical significance of the measurements in the analysis after etching with the Beraha's reagent is higher than in the analysis by the manual point count method.

Measurement accuracy is confirmed by the results of XRD of the same specimens that were quantified by the metallographic method. Figure 4 shows examples of diffraction patterns for samples of Steel 2, quenched from 1050 °C and 1250 °C, respectively. According to XRD, 51% and 22% of austenite was found in the specimens quenched from 1050 °C and 1250 °C, respectively.

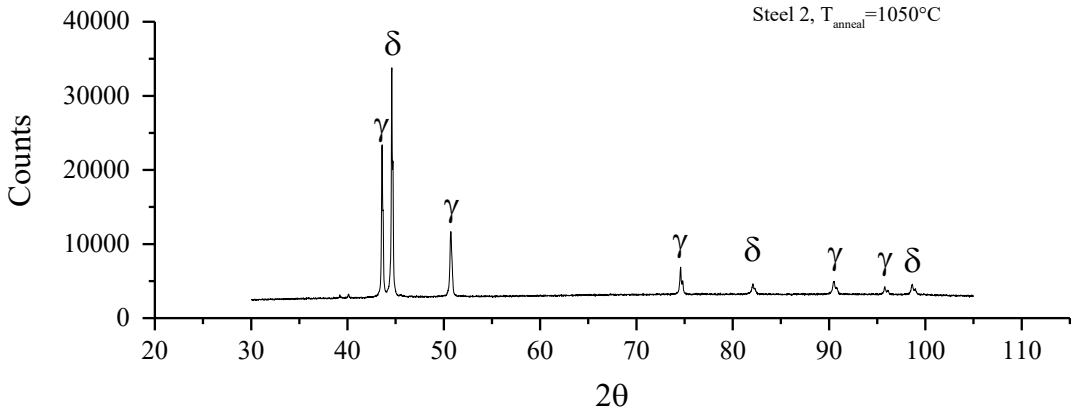

a

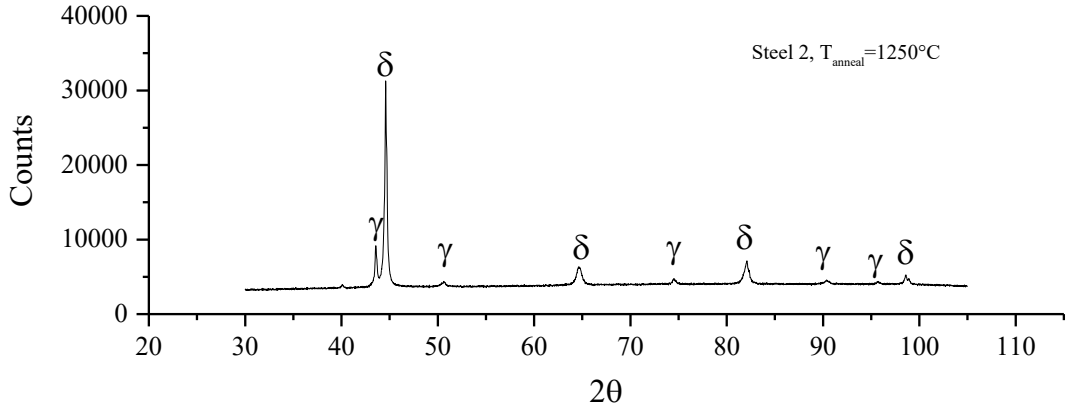

b

Figure 4. Diffraction patterns of the Steel 2: specimen quenched from 1050 °C (a) and 1250 °C (b)

To test the method for quantifying the σ-phase specimens of Steel 4, quenched from 1050 °C and annealed at 850 °C, were investigated. The results shown in Table 5 are consistent with the

data on the kinetics of the σ-phase [18]. Upon annealing for 60 minutes, the proportion of the σ-phase increases slightly to a content of about 17.4-20.4%, and then its proportion abruptly increases to 57.2%.

Table 5 – The results of assessing the amount of phase components in specimens of Steel 4 after annealing at 850 °C

Holding time, min	Volume fraction, %		
	Austenite	Ferrite	σ-phase
15	62.4	17.2	20.4
30	64.2	18.4	17.4
60	42.8	-	57.2

Conclusions

A technique for quantitative assessment of the DSS's microstructure based on etching with the Beraha's etchant solution and subsequent analysis of the content of austenite, ferrite, and σ-phase using the ASTM E 1245 method was developed. Analysis of a large number of other etchants showed that they are not suitable for the investigated steels.

Using a scanning electron microscope, the composition of the phases in the investigated specimens was determined. The phases were identified and compared with the structure observed with an optical light microscope.

It is shown that the results of measurements after etching with Beraha's etchant correlates with thermodynamic calculations and with measurements obtained using XRD. It is possible to use the developed technique as a basis for the development of new compositions and technology for the production of DSSs.

References

1. Topolska, S., & Łabanowski, J. (2009). Effect of microstructure on impact toughness of duplex and superduplex stainless steels. *Journal of Achievements in Materials and Manufacturing Engineering*, *36*(2), 142-149.
2. Cojocaru, E. M., Raducanu, D., Nocivin, A., Cinca, I., Vintila, A. N., Serban, N., Cojocaru, V. D. (2020). Influence of Aging Treatment on Microstructure and Tensile Properties of a Hot Deformed UNS S32750 Super Duplex Stainless Steel (SDSS) Alloy. *Metals*, *10*(3), 353.
3. Davanageri, M. B., Narendranath, S., & Kadoli, R. (2015). Influence of heat treatment on microstructure, hardness and wear behavior of super duplex stainless steel AISI 2507. *American Journal of Materials Science*, *5*(3C), 48-52.

4. Forgas Júnior, A., Otubo, J., & Magnabosco, R. (2016). Ferrite quantification methodologies for duplex stainless steel. *Journal of Aerospace Technology and Management*, *8*(3), 357-362.
5. "Standard Test Methods for Determining Average Grain Size." ASTM E112.
6. "Standard Practice for Determining the Inclusion or Second-Phase Constituent Content of Metals by Automatic Image Analysis", ASTM E 1245-03.
7. "Standard Practice for Assessing the Degree of Banding or Orientation of Microstructures." ASTM E1268.
8. Kazakov, A. A., Zhitenev, A. I., Fedorov, A. S., & Fomina, O. V. (2019). Development of duplex stainless steels Compositions. *CIS Iron and Steel Review*, *18*, 20-26.
9. Martins, M., & Casteletti, L. C. (2009). Sigma phase morphologies in cast and aged super duplex stainless steel. *Materials Characterization*, *60*(8), 792-795.
10. Andersson, J. O., Helander, T., Höglund, L., Shi, P., & Sundman, B. (2002). Thermo-Calc & DICTRA, computational tools for materials science. *Calphad*, *26*(2), 273-312.
11. Michalska, J., & Sozańska, M. (2006). Qualitative and quantitative analysis of σ and χ phases in 2205 duplex stainless steel. *Materials Characterization*, *56*(4-5), 355-362.
12. Llorca-Isern, N., López-Luque, H., López-Jiménez, I., & Biezma, M. V. (2016). Identification of sigma and chi phases in duplex stainless steels. *Materials Characterization*, *112*, 20-29.
13. Fedorov, A., Zhitenev, A., & Strekalovskaya, D. (2021). Effect of heat treatment on the microstructure and corrosion properties of cast duplex stainless steels. In *E3S Web of Conferences* (Vol. 225, p. 01003). EDP Sciences.
14. Vander Voort, G. F., & Manilova, E. P. (2005). Hints for imaging phases in steels. *Advanced materials & processes*, *163*(2), 32-37.
15. "Standard Test Method for Detecting Detrimental Phases in Lean Duplex Austenitic/ Ferritic Stainless Steels." ASTM A1084
16. Calliari, I., Zanesco, M., Bassani, P., & Ramous, E. (2009). Analysis of secondary phases precipitation in duplex stainless steels.
17. "Standard test method for determining volume fraction by systematic manual point count." ASTM E562.
18. Magnabosco, R. (2009). Kinetics of sigma phase formation in a duplex stainless steel. *Materials Research*, *12*(3), 321-327.